Available online at www.sciencedirect.com
ScienceDirect
Journal of the European Ceramic Society 27 (2007) 3907–3909
www.elsevier.com/locate/jeurceramsoc

Advances in the study of the conduction modes in SnO_2 varistors

R. Parra*, M.A. Ponce, C.M. Aldao, M.S. Castro

Institute of Materials Science and Technology (INTEMA), CONICET-UNMdP, J.B. Justo 4302, B7608FDQ-Mar del Plata, Argentina

Available online 26 March 2007

Abstract

The microstructure and electrical properties of the $SnO_2Co_3O_4Nb_2O_5La_2O_3$ varistor system prepared through the conventional mixed oxides route were characterised. The electrical breakdown field (E_r) and the non-linear coefficient (α) were determined from current density versus electric field curves. The barrier height and the concentration of donors were calculated by fitting the experimental data from impedance spectroscopy measurements assuming the formation of Schottky barriers at the grain boundaries and electrical conduction to occur due to tunnelling and thermionic emission. A model that takes into account the tunnelling contribution yielded more accurate results than a model based only on thermionic emission.

Keywords: Varistors; Electrical conductivity; Tunnelling

1. Introduction

Metal oxide varistors are electronic ceramic devices whose function is to sense and limit transient voltage surges and to do so repeatedly without being destroyed or damaged. If the voltage suddenly rises above the varistor breakdown voltage (E_r), it switches from a highly insulating state into a highly conducting state absorbing the excess of energy and preventing the equipment of interest from being damaged. Their non-linear current–voltage behaviour is strongly influenced by the addition of transition metal oxides to the varistor composition and by the nature of the atmosphere during sintering.[1–4]

Tin-dioxide varistors were reported for the first time in 1995 and have demonstrated many advantages over the successful ZnO varistors. Due to their higher electrical breakdown fields, SnO_2 varistors are suitable for high voltage applications as smaller devices. Furthermore, they have a higher thermal conductivity than varistors based on zinc oxide, which is an advantage concerning their stability towards thermal runaway.[5] The microstructure consists of a matrix of grains of SnO_2 with atomic defects such as positively charged donors ($V_O^{\bullet\bullet}$, $V_O^{\bullet}$, $Nb_{Sn}^{\bullet}$) located at the depletion layers and negatively charged acceptors (La'_{Sn}, Co'_{Sn}, Co''_{Sn}, V''_{Sn}, V''''_{Sn}, O', O'') at the grain boundaries interface.[3] Despite the promising advances made in the field, different opinions exist regarding the conduction mechanisms. Many authors propose the thermionic mechanism to be the one that controls the electrical conduction across Schottky type voltage barriers.[6] The purpose of the present work is to gain knowledge of the main conduction modes believed to control the electrical behaviour in SnO_2 varistors through the study of devices with a high non-linearity.

2. Experimental procedure

Analytical grades of SnO_2 (Aldrich), Co_3O_4 (Merck), Nb_2O_5 (Fluka AG), and La_2O_3 (Anedra) were used for processing SnO_2-based varistors. The selected composition here reported consisted of $(99.62 - x)$ mol% SnO_2 + 0.33 mol% Co_3O_4 + 0.05 mol% Nb_2O_5 + xLa_2O_3, with $x = 0$ (SCN), 0.05 (SCNL1) and 0.10 mol% (SCNL2). The composition corresponding to sample SCNL2 has demonstrated an excellent electrical response.[7] After mixing the powders in an alcoholic medium by stirring at 6000 rpm for 5 min, the slurries were kept at 65 °C for 48 h. The mixtures were sieved through a 43 μm mesh screen and the granulated powders were pressed into discs of a diameter of 12 mm and a thickness around 1 mm by uniaxial pressing (150 kg/cm^2). Finally, the discs were sintered in air at 1300 °C for 2 h with heating and cooling rates of 3 °C/min. In order to avoid or minimize Co loss during sintering and to ensure the desired composition, the discs were covered with their own powder.

The apparent density of the sintered samples was estimated by the Archimedes method. X-ray powder diffraction (XRD)

* Corresponding author.
E-mail address: rparra@fi.mdp.edu.ar (R. Parra).

0955-2219/$ – see front matter © 2007 Elsevier Ltd. All rights reserved.
doi:10.1016/j.jeurceramsoc.2007.02.060

analyses were carried out with a Philips 1830/00 equipment running with Co Kα radiation. The microstructural characterisation was performed by scanning electron microscopy (SEM) in a Topcon SM300 microscope. Silver electrodes were deposited on both faces of the sintered discs in order to study their electrical responses. The current density (J) versus electric field (E) characteristics were registered with a Keithley 237 source-meter unit. Impedance spectroscopy (IS) measurements were carried out by means of an HP 4284A LRC meter with an amplitude voltage of 0.5 V in the frequency range of 20 Hz–1 MHz. Due to the high resistivity of the studied specimens, IS measurements were performed at 150 °C. In order to avoid the possible influence of deep bulk traps, the grain boundary capacitance (C_{gb}) and resistance (R_{gb}) were obtained from plots of the capacitance (C_p) and the resistance (R_p) versus frequency (ν) from the high and low frequency limits, respectively.

3. Results and discussion

The X-ray powder diffraction patterns of the sintered samples showed no other phase besides cassiterite, suggesting single phase systems within the detection limits of this technique. Densities above 98% of the SnO_2 theoretical density (6.25 g/cm^3), and average grain sizes of approximately 5 μm, were measured.

Fig. 1 shows the J–E characteristics. The addition and subsequent increase in the content of La_2O_3 improved the varistor behaviour. As shown in Table 1, the sample with 0.10 mol% of La_2O_3 displayed the highest E_r and α. Fig. 2 shows the capacitance and resistance versus ν curves from which the C_{gb} and R_{gb} were determined. The obtained values are listed in Table 1. The

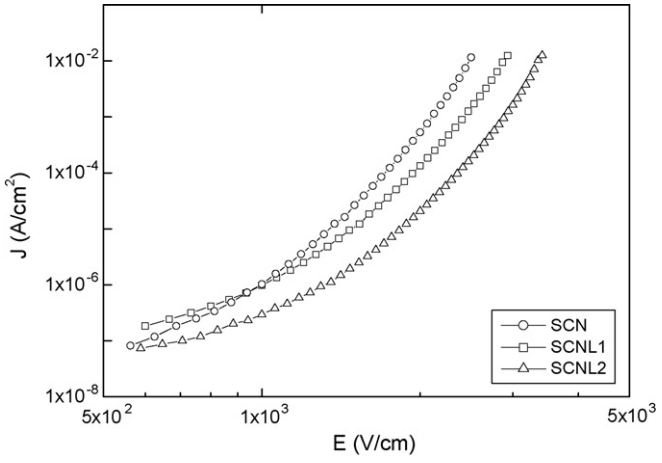

Fig. 1. J–E characteristic curves obtained at room temperature.

Table 1
Electric breakdown field (E_r), non-linearity coefficient (α) and grain boundary resistance (R_{gb}) and capacitance (C_{gb}) for sintered samples

	E_r (V/cm) at 1 mA/cm^2	α	R_{gb} (Ω) at 150 °C	C_{gb} (F) at 150 °C
SCN	2090	14	5.35×10^5	1.24×10^{-9}
SCNL1	2430	13	5.40×10^5	1.03×10^{-9}
SCNL2	2900	17	4.03×10^6	6.58×10^{-10}

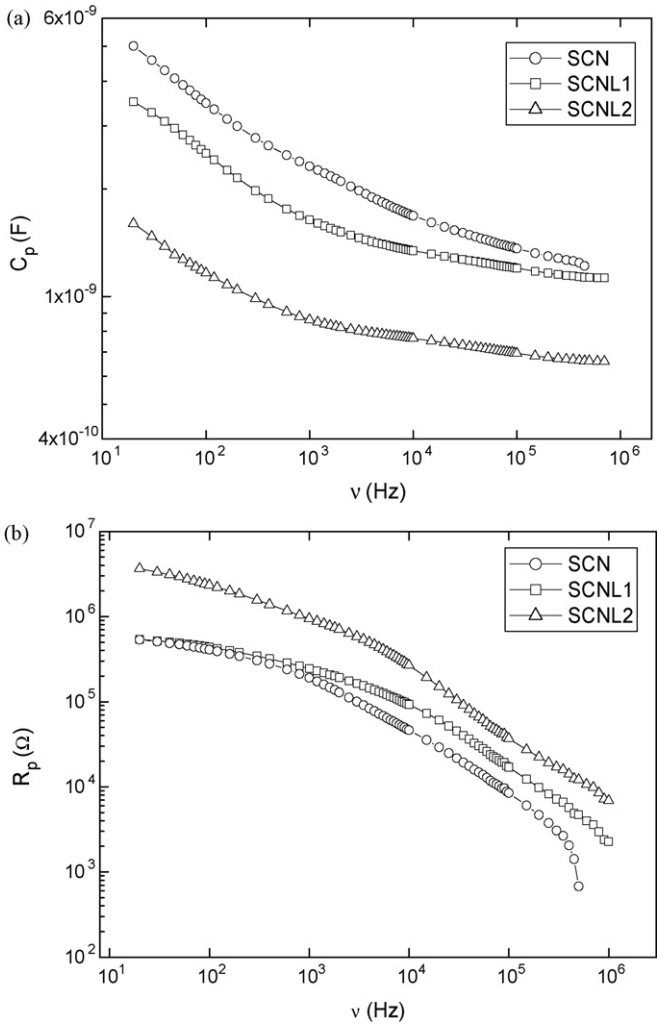

Fig. 2. Curves of the (a) capacitance and (b) resistance vs. ν registered at 150 °C.

higher E_r of sample SCNL2 is associated with its higher R_{gb} with respect to that of samples SCN and SCNL1. The enhancement of the electrical response of sample SCNL2 can be attributed to a higher segregation of atomic defects at grain boundaries. Due to their huge ionic volume with respect to that of Sn^{4+}, lanthanum ions most probably remain at grain boundaries and contribute to the development of effective intergranular voltage barriers.

Usually, quantitative descriptions of the potential barriers at grain boundaries are achieved after the thermionic approximation. The reported values of barrier height (ϕ) and donors concentration (N_d) thus obtained for tin dioxide varistors are around 1 eV and 10^{24} m^{-3}, respectively.[8] First, let us consider that the electrical conduction occurs by a purely thermionic mechanism. If so, values of barrier height and donor concentration can be obtained from the following expressions of the total current (J_{Total}) and the inverse of the grain boundary capacitance ($1/C_{gb}$),

$$J_{Total} = J_{therm.} = AT^2 \exp(-\phi/kT) \quad (1)$$

$$\frac{1}{C_{gb}} = 2\left(\frac{2n^2\phi}{q\varepsilon_0\varepsilon_r N_d S^2}\right)^{1/2}, \quad (2)$$

where A and k are the Richardson and Boltzmann constants, respectively, T the absolute temperature, n the average number of grains across the specimen thickness, q the electron charge, ε_0 the vacuum permittivity, ε_r the relative permittivity of SnO_2 and S is the area of the electrodes.[9] The results shown in Table 2 are in good agreement with those found in the literature.[8] Furthermore, as expected, the highest voltage barrier was obtained with sample SCNL2.

If the total current is now considered to be due to both tunnelling and thermionic emission, it would be expressed by

$$J_{\text{Total}} = J_{\text{tun.}} + J_{\text{therm.}} \tag{3}$$

or,

$$J_{\text{Total}} = \frac{AT}{k}\int_0^{\phi} f(E)P(E)\,\mathrm{d}E + AT^2\exp(-\phi/kT), \tag{4}$$

where $f(E)$ is the Fermi–Dirac distribution and $P(E)$ is the transmission probability for a reverse-biased Schottky barrier given by

$$P(E) = \exp - \left[\frac{4\pi\phi}{qh}\left(\frac{m\varepsilon}{N_{\text{d}}}\right)^{1/2} \ln\left(1 - \frac{(1-\beta)^{1/2}}{\beta^{1/2}}\right)\right], \tag{5}$$

where m is the electron effective mass ($0.3m_e$) and β is E/ϕ.[10,11] The ϕ and N_d values shown in Table 2 were determined through computational simulation by fitting the IS data with a double barrier model at grain boundaries while taking into account the dependence of N_d with ϕ according to Eq. (2). The greater changes are found in the donor concentration whereas the barrier height remains almost constant. Although higher values of barrier height and donor concentrations result when the combination of both conduction modes is considered, the differences may appear to be irrelevant at first glance.

Interestingly, if the ϕ and N_d values obtained through the *thermionic plus tunnelling* model are used to estimate both contributions to the total current separately, it can be seen in Table 3 that the current due to tunnelling exceeds in several orders of magnitude that of the thermionic current. Therefore, the tunnelling contribution cannot be neglected. To date, the thermionic conduction mode has been the most studied conduction mechanism in SnO_2 varistors. However, tunnelling through the barriers must be taken into account if a satisfactory explanation of the physics of electrical conduction in n-type semiconductors is desired.

Table 2
Voltage barrier height (ϕ) and donors concentration (N_d) obtained through different approaches to the electrical conduction

	Thermionic conduction		Thermionic plus tunnelling	
	ϕ (eV)	N_d (m^{-3})	ϕ (eV)	N_d (m^{-3})
SCN	0.96	4.88×10^{24}	1.16	5.31×10^{24}
SCNL1	0.96	3.37×10^{24}	1.13	3.74×10^{24}
SCNL2	1.03	1.48×10^{24}	1.14	1.54×10^{24}

Table 3
Predicted thermionic ($J_{\text{therm.}}$), tunnelling ($J_{\text{tun.}}$) and total current densities (J_{Total}) that result from considering the thermionic plus tunnelling conduction mode (see Table 2)

	$J_{\text{therm.}}$ (A/cm^2)	$J_{\text{tun.}}$ (A/cm^2)	J_{Total} (A/cm^2)
SCN	8.71×10^{-8}	2.40×10^{-5}	2.40×10^{-5}
SCNL1	2.54×10^{-7}	2.30×10^{-5}	2.32×10^{-5}
SCNL2	1.83×10^{-7}	2.91×10^{-6}	3.10×10^{-6}

Experimental total current densities: 2.38×10^{-5} A/cm^2 (SCN), 2.36×10^{-5} A/cm^2 (SCNL1) and 3.16×10^{-6} A/cm^2 (SCNL2).

4. Conclusions

We conclude that although the purely thermionic conduction mode leads to reasonable values of voltage barrier height and donors concentration, it constitutes an unsatisfactory model to describe the electrical conduction in SnO_2 varistors. Tunnelling through the barriers must be considered if an accurate characterisation of the voltage barrier features is sought. Furthermore, the contribution due to tunnelling across Schottky-type barriers was determined to be almost an order of magnitude higher than the thermally assisted current.

Acknowledgements

This research was financially supported by the National Research Council (CONICET) and by the University of Mar del Plata (UNMdP). R.P. wishes to thank the disinterested collaboration of Hernán Romeo. M.S.C. and R.P. also acknowledge the PROALERTA Project PI.VIII-13 (Cyted Program) for the financial aid during their presence at the Electroceramics X.

References

1. Levinson, L. M. and Philipp, H. M., Zinc-oxide varistors. A review. *Am. Ceram. Soc. Bull.*, 1986, **65**, 639–646.
2. Matsuoka, M., *Grain boundary phenomena in electronic ceramics, advances in ceramics*, *vol 1*, ed. L. M. Levinson. The American Ceramic Society Inc., Ohio, 1981, pp. 290–380.
3. Gupta, T. K., Application of zinc oxide varistors. *J. Am. Ceram. Soc.*, 1990, **73**, 1818–1840.
4. Clarke, D. R., Varistor ceramics. *J. Am. Ceram. Soc.*, 1999, **82**, 485–502.
5. Bueno, P. R., Varela, J. A., Barrado, C. M., Longo, E. and Leite, E. R., A comparative study of the thermal conductivity in ZnO- and SnO_2-based varistor systems. *J. Am. Ceram. Soc.*, 2005, **88**, 2629–2631.
6. Leite, E. R., Nascimento, A. M., Bueno, P. R., Longo, E. and Varela, J. A., The influence of sintering process and atmosphere on the non-ohmic properties of SnO_2 based varistors. *J. Mater. Sci.: Mater. Electron.*, 1999, **10**, 321–327.
7. Oliveira, M. M., Bueno, P. R., Cassia-Santos, M. R., Longo, E. and Varela, J. A., Sensitivity of SnO_2 non-ohmic behaviour to the sintering process and to the addition of La_2O_3. *J. Eur. Ceram. Soc.*, 2001, **21**, 1179–1185.
8. Bueno, P. R., de Cassia-Santos, M. R., Leite, E. R., Longo, E., Bisqert, J., Garcia-Belmonte, G. *et al.*, Nature of the Schottky-type barrier of highly dense SnO_2 systems displaying nonohmic behavior. *J. Appl. Phys.*, 2000, **88**, 1–4.
9. Castro, M. S. and Aldao, C. M., Thermionic, tunnelling and polarization currents in zinc oxide varistors. *J. Eur. Ceram. Soc.*, 1997, **17**, 1533–1537.
10. Robertson, J., Defect levels of SnO_2. *Phys. Rev. B*, 1984, **30**, 3520–3522.
11. Castro, M. S. and Aldao, C. M., Prebreakdown conduction in zinc oxide varistors: thermionic or tunnel currents and one-step or two-step conduction processes. *Appl. Phys. Lett.*, 1993, **63**, 1077–1079.